Data-Aided Symbol Timing and CFO Synchronization for Filter Bank Multicarrier Systems

Tilde Fusco, Angelo Petrella, and Mario Tanda

***Abstract*—In this paper we consider the problem of data-aided joint symbol timing and carrier-frequency offset (CFO) estimation for filter bank-based multicarrier (FBMC) systems. As all multicarrier systems, FBMC systems are very sensitive to synchronization errors, since CFO and symbol timing errors cause interference between successive symbols and adjacent subcarriers which can lead to a severe performance degradation. Therefore, reliable and accurate synchronization algorithms must be designed for these systems. The approach herein presented is based on the deployment of appropriate training sequences. In particular, we propose a new joint symbol timing and CFO synchronization algorithm based on the least squares approach and exploiting the transmission of a training sequence made up of identical parts. The performance of the derived estimators, assessed by computer simulations, is compared with that of two data-aided synchronization algorithms previously proposed in the literature.**

***Index Terms*—Data-aided estimation, carrier-frequency offset, symbol timing, filter bank multicarrier systems.**

I. Introduction

RECENTLY, filter bank multicarrier (FBMC) systems have received considerable attention for wired and wireless high-data-rate transmissions in frequency selective channels. Differently from conventional multicarrier systems, known as orthogonal frequency division multiplexing (OFDM) systems, FBMC systems employ bandlimited pulse shaping filters that overlap in time. This involves several advantages such as reduced sensitivity to narrowband interference, high flexibility to allocate group of subchannels to different users and an high spectral containment. FBMC systems referred to as Filtered Multitone (FMT) systems have been proposed for very high-speed digital subscriber line (VDSL) standards [1] and are under investigation also for broadband wireless applications [2], [3]. FBMC systems based on offset QAM modulation (OQAM), known as OFDM/OQAM systems, have been considered by the 3GPP standardization forum for improved downlink UTRAN interfaces [4].

Manuscript received June 30, 2008; revised November 28, 2008; accepted January 26, 2009. The associate editor coordinating the review of this paper and approving it for publication was Y.-C. Ko.

The authors are with the Dipartimento di Ingegneria Biomedica, Elettronica e delle Telecomunicazioni, Università di Napoli Federico II, via Claudio 21, I-80125 Napoli, Italy (e-mail: mario.tanda@unina.it).

This work was presented in part at the 2008 European Signal Processing Conference (EUSIPCO 2008), August 2008, Lausanne, Switzerland.

This work was supported in part by the European Commission under Project PHYDYAS (FP7-ICT-2007-1-211887).

Digital Object Identifier 10.1109/TWC.2009.080860

However, one of the major disadvantages of FBMC systems is their sensitivity to carrier frequency and symbol timing errors. Specifically, as investigated in [5] and in [6] phase noise and misalignments in time and frequency can considerably degrade the performance of FMT and OFDM/OQAM systems, giving rise to interference between successive symbols and adjacent subcarriers. Therefore, reliable and accurate symbol timing and carrier-frequency offset (CFO) synchronization schemes must be designed for these systems.

Recently, data-aided and non-data-aided (or blind) synchronization algorithms for FBMC systems have been considered. Specifically, in [7] it is presented a blind joint CFO and symbol timing estimator exploiting the unconjugate cyclostationarity of the received OFDM/OQAM signal while, in [8] it is shown that accurate CFO estimation algorithms can be obtained by using both the conjugate and the unconjugate cyclostationarity properties of the received OFDM/OQAM signal. The conjugate and unconjugate correlation functions of the pulse shaping OFDM/OQAM signal have been also used in [9] to derive blind CFO estimators based on the maximum-likelihood (ML) principle and obtained under the hypothesis of low signal-to-noise (SNR) ratio. In [10] a blind closed-form CFO estimator for FMT systems based on the best linear unbiased estimation principle with remarkable robustness against multipath fading has been proposed. Moreover, in [11] are derived data-aided joint symbol timing and frequency offset synchronization schemes in the time domain for FMT systems while, in [12] the problem of data-aided synchronization and channel estimation in the frequency domain for OFDM/OQAM systems is considered.

Inspired to these works we develop in this paper a synchronization scheme for data-aided symbol timing and frequency offset recovery with robust acquisition properties in dispersive channels. Specifically, we consider an algorithm based on the least squares (LS) approach which exploits the known structure of a training sequence made up of identical parts. The proposed method, as illustrated by numerical simulations, can assure in a multipath channel sufficiently accurate symbol timing and CFO estimates.

The organization of this paper is as follows. In Section II we describe the considered FBMC system model, investigating the effects of time and frequency synchronization errors. In Section III we derive the proposed joint symbol timing and CFO estimator. The Cramér-Rao vector bound (CRVB) of symbol timing, CFO and phase offset estimation for the

problem at the hand is derived in Section IV. Numerical results are presented in Section V and conclusions are drawn in the final Section.

Notation: $j \triangleq \sqrt{-1}$, superscript $(\cdot)^*$ denotes the complex conjugation, $\Re[\cdot]$ real part, $\Im[\cdot]$ imaginary part, $|\cdot|$ absolute value and $\angle[\cdot]$ the argument of a complex number in $[-\pi, \pi)$, $lcm\{a, b\}$ is the least common multiple between a and b, $\delta(t)$ the Dirac delta and $\otimes$ is the discrete-time convolution operator. Moreover, $(\cdot)^T$ indicates transpose, $(\cdot)^H$ Hermitian, $(\cdot)^{-1}$ the inverse of a matrix, $\boldsymbol{I}_n$ is an $n \times n$ identity, $\mathrm{diag}\{\cdot\}$ is a diagonal matrix, while $E[\cdot]$ stands for the statistical expectation, $\mathcal{O}$ is the Landau symbol and $\lfloor \cdot \rfloor$ denotes the floor operator that rounds its argument to the near integer towards minus infinity. Finally, lower (upper) case boldface symbols denote column vectors (matrices).

II. FBMC System Model

A. OFDM/OQAM System Model With Synchronization Errors

Let us consider an OFDM/OQAM system with N subcarriers of which N_u are modulated by data symbols and $N_v = N - N_u$ remain unmodulated (virtual subcarriers). As indicated in Fig. 1, the real and imaginary parts of the transmitted complex data symbol $a_l^R(p)$ and $a_l^I(p)$ are separated in time by $T/2$ and transmitted in parallel on the N subchannels. Each subchannel is then shaped by a prototype filter with impulse response $g(t)$ and successively the N contributes are summed up giving the $T_s = T/N$ sampled multicarrier signal

$$\begin{aligned} s(kT_s) = \quad & \sqrt{\frac{N}{2N_u}} \sum_{p=-\infty}^{\infty} \sum_{l \in \mathcal{A}} e^{jl\left(\frac{2\pi}{T} kT_s + \frac{\pi}{2}\right)} \\ & \times \left[a_l^R(p) g(kT_s - pNT_s) \right. \\ & \left. + j a_l^I(p) g\left(kT_s - NT_s/2 - pNT_s\right) \right] . \end{aligned} \tag{1}$$

In (1) $\mathcal{A}$ denotes the set of indices of data subcarriers, T is the signaling interval and $g(t)$ is the real pulse-shaping filter with unit energy and assumed to be a square-root raised cosine (SRRC) Nyquist filter with a roll-off factor α $(0 \leq \alpha \leq 1)$.

The transmitted sequence $s(kT_s)$ feeds a digital-to-analog converter (DAC) and propagates trough a physical channel characterized by AWGN noise $n(t)$ with a power spectral density $S_n(f) = \sigma_n^2$. The received signal $r(t)$ is filtered with an ideal low-pass filter with a bandwidth of $1/T_s$ and sampled with a frequency $f_s = 1/T_s$, yielding the sequence

$$r(kT_s) = e^{j(2\pi \Delta f T_s k + \phi)} s(kT_s - \tau) + n(kT_s) \tag{2}$$

where τ is the timing offset, Δf the CFO and ϕ the carrier phase offset, moreover, $n(kT_s)$ denotes the zero-mean circular complex white Gaussian noise with a variance σ_n^2/T_s.

In subchannel m at the receiver side, the received sequence $r(kT_s)$ is first down-converted by multiplying with $e^{-j\left(\frac{2\pi}{T} kT_s + \frac{\pi}{2}\right)m}$, then filtered by the matched filter $\tilde{g}(kT_s)$ to generate the signal

$$y_m(kT_s) = r(kT_s) e^{-j\left(\frac{2\pi}{T} kT_s + \frac{\pi}{2}\right)m} \otimes \tilde{g}(kT_s) . \tag{3}$$

Down-sampling by $N/2$ times the received subchannel sequence $y_m(kT_s)$ and taking the real and imaginary parts alternately, we get the received symbols:

$$\tilde{a}_m^R(k) = \Re\left\{ y_m(qT_s)|_{q=kN} \right\} \tag{4}$$

$$\tilde{a}_m^I(k) = \Im\left\{ y_m(qT_s)|_{q=kN+N/2} \right\} . \tag{5}$$

Substituting (3) in (4) and (5) and accounting for the expression of the received signal we obtain

$$\begin{aligned} & \tilde{a}_m^R(k) = \Re\left\{ r(qT_s) e^{-j\left(\frac{2\pi}{T} qT_s + \frac{\pi}{2}\right)m} \otimes \tilde{g}(qT_s) \Big|_{q=kN} \right\} \\ & = a_m^R(k) \Re\left\{ p_{m,m}^{\Delta f}(-\tau) e^{j\left(\phi - \frac{2\pi}{T}\tau m\right)} \right\} \\ & + \sum_{\substack{m' \in \mathcal{A} \\ m' \neq m}} a_{m'}^R(k) \Re\left\{ p_{m',m}^{\Delta f}(-\tau) e^{j\left(\phi - \frac{2\pi}{T}\tau m\right)} \right\} \\ & + \sum_{m' \in \mathcal{A}} \sum_{\substack{k' = -\infty \\ k' \neq k}}^{\infty} a_{m'}^R(k') \\ & \times \Re\left\{ p_{m',m}^{\Delta f}((k-k')NT_s - \tau) e^{j\left(\phi - \frac{2\pi}{T}\tau m\right)} \right\} \\ & - \sum_{m' \in \mathcal{A}} \sum_{k'=-\infty}^{\infty} a_{m'}^I(k') \\ & \times \Im\left\{ p_{m',m}^{\Delta f}((k-k')NT_s - NT_s/2 - \tau) e^{j\left(\phi - \frac{2\pi}{T}\tau m\right)} \right\} \\ & + \Re\left\{ n(qT_s) e^{-j\left(\frac{2\pi}{T} qT_s + \frac{\pi}{2}\right)m} \otimes \tilde{g}(qT_s) \Big|_{q=kN} \right\} \end{aligned} \tag{6}$$

and

$$\begin{aligned} & \tilde{a}_m^I(k) = \Im\left\{ r(qT_s) e^{-j\left(\frac{2\pi}{T} qT_s + \frac{\pi}{2}\right)m} \otimes \tilde{g}(qT_s) \Big|_{q=kN+N/2} \right\} \\ & = a_m^I(k) \Re\left\{ \breve{p}_{m,m}^{\Delta f}(-\tau) e^{j\left(\phi - \frac{2\pi}{T}\tau m\right)} \right\} \\ & + \sum_{\substack{m' \in \mathcal{A} \\ m' \neq m}} a_{m'}^I(k) \Re\left\{ \breve{p}_{m',m}^{\Delta f}(-\tau) e^{j\left(\phi - \frac{2\pi}{T}\tau m\right)} \right\} \\ & + \sum_{m' \in \mathcal{A}} \sum_{\substack{k' = -\infty \\ k \neq k'}}^{\infty} a_{m'}^I(k') \\ & \times \Re\left\{ \breve{p}_{m',m}^{\Delta f}((k-k')NT_s - \tau) e^{j\left(\phi - \frac{2\pi}{T}\tau m\right)} \right\} \\ & + \sum_{m' \in \mathcal{A}} \sum_{k'=-\infty}^{\infty} a_{m'}^R(k') \\ & \times \Im\left\{ \breve{p}_{m',m}^{\Delta f}((k-k')NT_s + NT_s/2 - \tau) e^{j\left(\phi - \frac{2\pi}{T}\tau m\right)} \right\} \\ & + \Im\left\{ n(qT_s) e^{-j\left(\frac{2\pi}{T} qT_s + \frac{\pi}{2}\right)m} \otimes \tilde{g}(qT_s) \Big|_{q=kN+N/2} \right\} \end{aligned} \tag{7}$$

where

$$\begin{aligned} & p_{m',m}^{\Delta f}((k-k')NT_s - \tau) \triangleq \sqrt{\frac{N}{2N_u}} j^{m'-m} \\ & \times \left[\tilde{g}(qT_s) \otimes e^{j2\pi q\left(\Delta f T_s + \frac{m'-m}{N}\right)} g(qT_s - k'NT_s - \tau) \right] \Big|_{q=kN} \end{aligned} \tag{8}$$

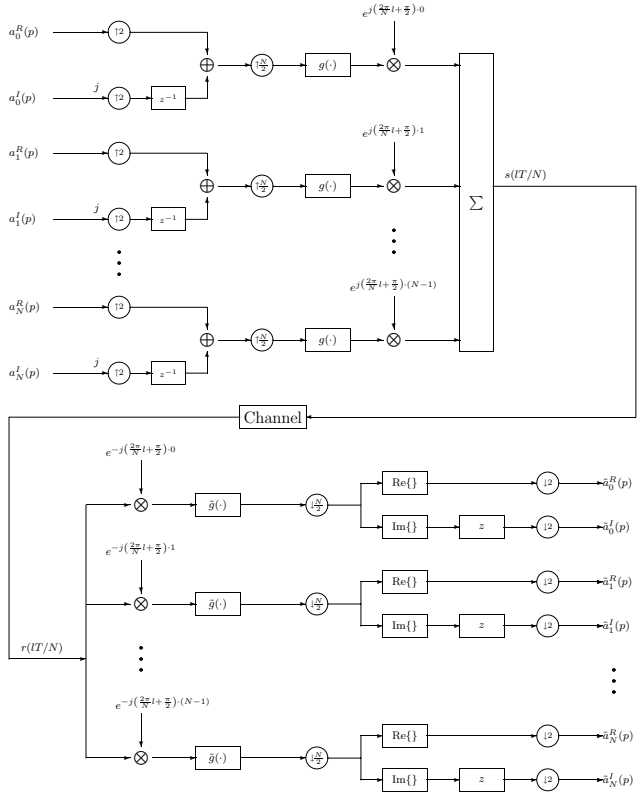

Fig. 1. OFDM/OQAM system.

$$\breve{p}^{\Delta f}_{m',m}((k-k')NT_s-\tau) \triangleq \sqrt{\frac{N}{2N_u}} j^{m'-m}\Big[\tilde{g}(qT_s) \otimes e^{j2\pi q\left(\Delta f T_s+\frac{m'-m}{N}\right)} g(qT_s-k'NT_s-\tau)\Big]\Big|_{q=kN+N/2} \tag{9}$$

From (6) and (7) we can note that in the presence of frequency and timing synchronization errors the useful term is subject to an attenuation and a phase rotation related to the subchannel index m, the timing offset τ, the phase offset ϕ, the CFO Δf and the index of the information symbol k. Furthermore, intercarrier interference, intersymbol interference and interference between real and imaginary part of data symbols are present.

B. FMT System Model With Synchronization Errors

Into the case of an FMT system, as shown in Fig.2, the baseband discrete-time transmitted signal obtained by sampling the continuous-time signal with a sampling frequency $f_s{=}1/T_s{=}K/T$ is given by

$$s(kT_s) \;= \sqrt{\frac{K}{N_u}} \sum_{p=-\infty}^{\infty} \sum_{l\in\mathcal{A}} a_l(p) g\left(kT_s - pT\right) e^{j2\pi \frac{K}{NT} lkT_s} \tag{10}$$

where T is the signaling interval, $K \triangleq N(1+\alpha)$ is the oversampling factor, $a_l(p)$ is the data symbol transmitted on the lth subcarrier of the pth FMT symbol and $g(t)$ is the real prototype filter with unit energy and assumed to be an SRRC Nyquist filter with a roll-off factor $\alpha = (K-N)/N$ $(0 \le \alpha \le 1)$. We can note that, differently from OFDM/OQAM systems, for FMT systems the frequency spacing between adjacent subcarriers is given by $K/(NT) = (1+\alpha)/T$ and, thus, it depends on the oversampling factor. Precisely, if the oversampling factor is equal to the number of subcarriers $K = N$ the system is referred to as critically sampled FMT system and the frequency spacing is equal to $1/T$. Otherwise when $\alpha > 0$ the system is referred to as non-critically sampled FMT system and the frequency spacing increases minimizing the amount of ICI at the price of an increment in the implementation complexity and of a reduction of bandwidth efficiency.

Let us suppose now that the FMT signal is transmitted through an AWGN channel. The received signal in the presence of a CFO Δf, a carrier phase offset ϕ and a timing offset τ, is given by

$$r(kT_s) = e^{j(2\pi\Delta f T_s k+\phi)} s(kT_s-\tau) + n(kT_s)\,. \tag{11}$$

At the receiver side the FMT signal is filtered with a bank of matched filters and downsampled of the factor K, thus, we obtain

$$\begin{aligned}\tilde{a}_m(k) =\; & r(qT_s)e^{-j\frac{2\pi}{T}m(1+\alpha)qT_s} \otimes \tilde{g}(qT_s)\Big|_{q=kK} \\ =\; & a_m(k)\; q^{\Delta f}_{m,m}(-\tau)e^{j\left[\phi-\frac{2\pi}{T}m(1+\alpha)\tau\right]} \\ & + \sum_{\substack{m'\in\mathcal{A}\\ m'\neq m}} a_{m'}(k)\; q^{\Delta f}_{m',m}(-\tau)e^{j\left[\phi-\frac{2\pi}{T}m(1+\alpha)\tau\right]} \\ & + \sum_{m'\in\mathcal{A}} \sum_{\substack{k'=-\infty\\ k\neq k'}}^{\infty} a_{m'}(k') \\ & \times q^{\Delta f}_{m',m}((k-k')KT_s-\tau)e^{j\left[\phi-\frac{2\pi}{T}m(1+\alpha)\tau\right]} \\ & + n(qT_s)e^{-j\frac{2\pi}{T}m(1+\alpha)qT_s} \otimes \tilde{g}(qT_s)\Big|_{q=kK}\end{aligned} \tag{12}$$

with

$$\begin{aligned}q^{\Delta f}_{m',m}((k-k')KT_s-\tau) \triangleq & \sqrt{\frac{K}{N_u}} \\ & \times e^{j2\pi q\left(\Delta f T_s+\frac{m'-m}{N}\right)} g(qT_s-k'KT_s-\tau) \otimes \tilde{g}(qT_s)\Big|_{q=kK}\,.\end{aligned} \tag{13}$$

Therefore, in the presence of synchronization errors and in the case of a non dispersive channel the useful term is subject to the attenuation and the phase rotation due to the term

$$\begin{aligned}q^{\Delta f}_{m,m}(-\tau)e^{j\left[\phi-\frac{2\pi}{T}m(1+\alpha)\tau\right]} &= \sqrt{\frac{K}{N_u}} e^{j\left[\phi-\frac{2\pi}{T}m(1+\alpha)\tau\right]} \\ & \times \left[e^{j2\pi\Delta f q T_s} g(qT_s-kKT_s-\tau) \otimes \tilde{g}(qT_s)\big|_{q=kK}\right] \\ &= \sqrt{\frac{K}{N_u}} e^{j\left(\phi-\frac{2\pi}{T}m(1+\alpha)\tau\right)} \\ & \times \sum_{p=-\infty}^{\infty} e^{j2\pi\Delta f(kKT_s-pT_s)} g(pT_s-\tau)g(pT_s)\end{aligned}$$

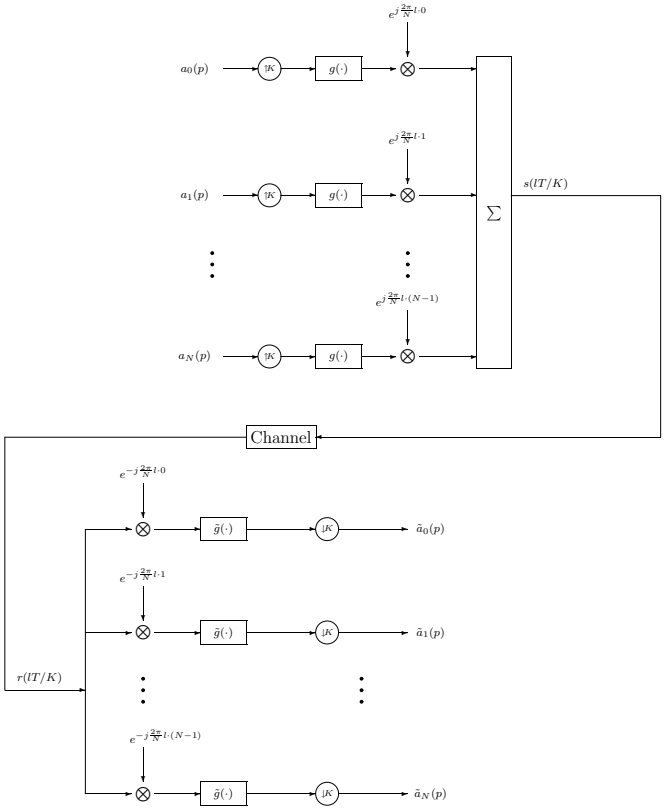

Fig. 2. FMT system.

and, moreover it is affected by ICI, ISI and additive noise.

III. Joint Symbol Timing and CFO LS Estimator

In this section we derive a data-aided joint CFO and symbol timing estimator based on the LS approach which exploits the transmission of a training sequence made up of identical blocks. Precisely, the training sequence can be obtained by transmitting the sequence of data symbols $a_l(p) = a_l^{TR}\ \forall l \in \mathcal{A}$ and $\forall p \in \{0, ..., N_{TR}-1\}$. In this way, if we assume that the pulse shaping filter $g(t)$ is different from zero for $t \in \{0, T_s, ..., (N_g-1)T_s\}$, where $N_g = \gamma\, T/T_s$ with γ the overlapping factor, we obtain the training burst

$$s_{TR}(kT_s) = \begin{cases} \sqrt{\dfrac{K}{N_u}} \displaystyle\sum_{l\in\mathcal{A}} a_l^{TR} e^{j\frac{2\pi}{N}kl} \sum_{p=0}^{N_{TR}-1} g\left(kT_s - pKT_s\right) \\ \text{FMT} \\ \\ \sqrt{\dfrac{N}{2N_u}} \displaystyle\sum_{p=0}^{N_{TR}-1} \sum_{l\in\mathcal{A}} e^{jl\left(\frac{2\pi}{N}k+\frac{\pi}{2}\right)} \Big[a_l^{R,TR} g(kT_s - pNT_s) \\ +ja_l^{I,TR} g\left(kT_s - NT_s/2 - pNT_s\right)\Big] \\ \text{OFDM/OQAM}\,. \end{cases} \tag{14}$$

After a transient of $N_g - 1$ samples and, in particular for $k \in \{N_g - 1, ..., N_{TR}N - P - 1\}$, the training sequence in (14) satisfies the following relationship

$$s_{TR}(kT_s + PT_s) = s_{TR}(kT_s) \tag{15}$$

with $P = lcm\{N, K\}$ for FMT systems and $P = N$ for OFDM/OQAM systems. Thus, the number of identical blocks contained in the training sequence is $N_{rip}^{OFDM/OQAM} = N_{TR} - \gamma$ for OFDM/OQAM systems while, for FMT systems the number of identical blocks is $N_{rip}^{FMT} = \left\lfloor \dfrac{N_{TR}N - \gamma K}{P} \right\rfloor$.

Accounting for the relationship (15) a joint symbol timing and CFO estimator can be obtained by considering the minimization problem

$$(\Delta\hat{f}, \hat{\tau}) = \arg\min_{\Delta\tilde{f},\tilde{\tau}} \left\{ \sum_{k=N_g-1}^{N_{TR}N-P-1} \left| r(kT_s + \tilde{\tau}) - r(kT_s + PT_s + \tilde{\tau}) e^{-j2\pi\Delta\tilde{f}T_s P} \right|^2 \right\} \tag{16}$$

where $\Delta\tilde{f}$ and $\tilde{\tau}$ are trial values for CFO and symbol timing, respectively. The minimization in (16) (see the algebraic details reported in Appendix A) leads to the following joint CFO and symbol timing estimator referred to as LS estimator

$$\hat{\tau}_{LS} = \arg\max_{\tilde{\tau}} \left\{ 2\left|R(\tilde{\tau})\right| - Q_1(\tilde{\tau}) - Q_2(\tilde{\tau}) \right\} \tag{17}$$

$$\Delta\hat{f}_{LS}(\hat{\tau}_{LS}) = \frac{1}{2\pi PT_s} \angle\left\{R(\hat{\tau}_{LS})\right\} \tag{18}$$

with

$$R(\tilde{\tau}) \stackrel{\triangle}{=} \sum_{k=N_g-1}^{N_{TR}N-P-1} r^*(kT_s + \tilde{\tau}) r(kT_s + PT_s + \tilde{\tau}) \tag{19}$$

and

$$Q_i(\tilde{\tau}) \stackrel{\triangle}{=} \sum_{k=N_g-1}^{N_{TR}N-P-1} \left| r(kT_s + (i-1)PT_s + \tilde{\tau}) \right|^2, \qquad i = 1, 2. \tag{20}$$

Let us observe that if we divide the timing metric in (17) by the term $Q(\tilde{\tau}) \stackrel{\triangle}{=} Q_1(\tilde{\tau}) + Q_2(\tilde{\tau})$ we obtain the modified LS (MLS) joint symbol timing and CFO estimator

$$\hat{\tau}_{MLS} = \arg\max_{\tilde{\tau}} \left\{ \frac{\left|R(\tilde{\tau})\right|}{Q(\tilde{\tau})} \right\} \tag{21}$$

$$\Delta\hat{f}_{MLS}(\hat{\tau}_{MLS}) = \frac{1}{2\pi PT_s} \angle\left\{R(\hat{\tau}_{MLS})\right\} \tag{22}$$

that can be used to reduce the false detection probability [13]. The performance of the LS and MLS estimators will be compared with that of the two joint estimators proposed by Tonello and Rossi in [11] and referred in the following as TR1 and TR2. Specifically, the joint estimator

$$\hat{\tau}_{TR1} = \arg\max_{\tilde{\tau}} \left\{ \frac{\left|R(\tilde{\tau})\right|^2}{Q_2(\tilde{\tau})^2} \right\} \tag{23}$$

$$\Delta\hat{f}_{TR1}(\hat{\tau}_{TR1}) = \frac{1}{2\pi PT_s} \angle\left\{R(\hat{\tau}_{TR1})\right\} \tag{24}$$

exploits only the periodicity of the training burst in (14), while the joint estimator

$$\hat{\tau}_{TR2} = \arg\max_{\tilde{\tau}} \left\{ \frac{\left|S(\tilde{\tau})\right|^2}{T(\tilde{\tau})^2} \right\} \tag{25}$$

$$\Delta\hat{f}_{TR2}(\hat{\tau}_{TR2}) = \frac{1}{2\pi PT_s}\angle\{S(\hat{\tau}_{TR2})\} \tag{26}$$

with

$$S(\tilde{\tau}) = \sum_{k=N_g-1}^{N_{TR}N-P-1} [r^*(kT_s+\tilde{\tau})s_{TR}(kT_s) \times r(kT_s+PT_s+\tilde{\tau})s^*_{TR}(kT_s+PT_s)] \tag{27}$$

and

$$T(\tilde{\tau}) = \sum_{k=N_g-1}^{N_{TR}N-P-1} |s_{TR}(kT_s)|^2|s_{TR}(kT_s+PT_s)|^2 \tag{28}$$

exploits also the knowledge of the periodic training burst. It is worthwhile to note that the considered LS, MLS, TR1 and TR2 CFO estimators in (18), (22), (24) and (26), respectively, provide a closed form solution for the CFO estimate and do not require the knowledge of the SNR. Moreover, in the case of OFDM/OQAM systems they can assure unambiguous CFO estimates if $|\Delta f T_s| < 1/(2N)$, while in the case of FMT systems their acquisition range is reduced to $|\Delta f T_s| < 1/(2P)$. On the other hand, the considered LS, MLS, TR1 and TR2 symbol timing estimators in (17), (21), (23) and (25), respectively, do not present a closed form solution but they require a maximization with respect to the continuous parameter $\tilde{\tau}$.

We underline that in the case of FMT systems the amount of redundancy needed to transmit the training sequence is greater than that exploited in the case of OFDM/OQAM systems. In fact, in the case of OFDM/OQAM systems the training sequence is composed by $N_{rip}^{OFDM/OQAM} = N_{TR} - \gamma$ identical OFDM/OQAM symbols of length N while, in the case of FMT systems, it is necessary to transmit a training sequence such that $N_{TR}N - \gamma K > P$, where $P = lcm\{N, K\}$ can be much greater than N.

IV. Cramér-Rao Bound

In this section we derive the expression of the CRVB for joint CFO, phase offset and symbol timing estimation for FBMC systems. Let $\boldsymbol{v} = [\tau, \Delta f, \phi]^T$ the set of parameters to be estimated and let us consider the observations vector of total length $W = N_{TR}N - N_g + 1$

$$\begin{aligned}\boldsymbol{r} &\triangleq [r(N_gT_s - T_s), ..., r(N_{TR}NT_s - T_s)]^T \\ &= \boldsymbol{\Psi}(\Delta f, \phi)\boldsymbol{s}(\tau) + \boldsymbol{n}\end{aligned}$$

with $\boldsymbol{s}(\tau) \triangleq [s(N_gT_s - T_s - \tau), ..., s(N_{TR}NT_s - T_s - \tau)]^T$ the vector of the transmitted training sequence, $\boldsymbol{\Psi}(\Delta f, \phi) \triangleq \mathrm{diag}\{e^{j[2\pi(N_g-1)T_s\Delta f+\phi]}, ..., e^{j[2\pi(N_{TR}NT_s-T_s)\Delta f+\phi]}\}$ and $\boldsymbol{n}$ the noise vector with zero mean and covariance matrix $\boldsymbol{C_n} = \frac{\sigma_n^2}{T_s}\boldsymbol{I}_W$. The (i,l)th entry of the Fisher Information Matrix (FIM) is equal to

$$[\boldsymbol{F}]_{(i,l)} = -\mathrm{E}\left[\frac{\partial \ln p(\boldsymbol{r}|\boldsymbol{v})}{\partial[\boldsymbol{v}]_i\,\partial[\boldsymbol{v}]_l}\right] \qquad \forall i,l \in \{1,2,3\} \tag{29}$$

where $\ln\{p(\boldsymbol{r}|\boldsymbol{v})\}$ is the logarithm of the probability density function of $\boldsymbol{r}$ whose expression (up to irrelevant additive factors) is given by

$$\begin{aligned}\ln\{p(\boldsymbol{r}|\boldsymbol{v})\} = &\frac{2T_s}{\sigma_n^2}\Re\left\{\boldsymbol{r}^*\boldsymbol{\Psi}(\Delta f,\phi)\boldsymbol{s}(\tau)^T\right\} \\ &-\frac{T_s}{\sigma_n^2}\boldsymbol{s}(\tau)\boldsymbol{s}(\tau)^H .\end{aligned} \tag{30}$$

Substituting (30) into (29) and taking the statistical expectation we obtain the elements of the FIM given in (31) shown at the top of the next page. with $\boldsymbol{D}_{\Delta f} \triangleq j2\pi T_s\mathrm{diag}\{N_g-1, \ldots, N_{TR}N-1\}$ and $\boldsymbol{D}_\phi \triangleq j\boldsymbol{I}_W$.

In the case of FMT systems by following the algebraic manipulations reported in Appendix B the CRVBs for symbol timing, CFO and phase offset estimation are given by

$$\begin{aligned}\mathrm{CRVB}(\tau) = &\left[\boldsymbol{F}^{-1}\right]_{(1,1)} \\ = &\frac{(NT_s)^2}{8\pi^2 W\mathrm{SNR}\left[\frac{1}{N_u}\sum_{l\in\mathcal{A}}\left(l - \frac{1}{N_u}\sum_{l\in\mathcal{A}} l\right)^2\right]}\end{aligned} \tag{32}$$

$$\mathrm{CRVB}(\Delta f) = \left[\boldsymbol{F}^{-1}\right]_{(2,2)} = \frac{3}{2(\pi T_s)^2\mathrm{SNR}\,W^3} \tag{33}$$

$$\begin{aligned}\mathrm{CRVB}(\phi) = &\left[\boldsymbol{F}^{-1}\right]_{(3,3)} \\ = &\frac{3\left[4\beta\frac{1}{N_u}\sum_{l\in\mathcal{A}} l^2 - W^2\left(\frac{1}{N_u}\sum_{l\in\mathcal{A}} l\right)^2\right]}{2W^3\mathrm{SNR}\left[\frac{1}{N_u}\sum_{l\in\mathcal{A}}\left(l - \frac{1}{N_u}\sum_{l\in\mathcal{A}} l\right)^2\right]}\end{aligned} \tag{34}$$

with $\beta \triangleq \frac{N_{TR}^2N^2 + N_{TR}NN_g - 4N_{TR}N + N_g^2 - 5N_g + 7}{3}$.

From (32), (33) and (34) we can note that the derived CRVBs are inversely proportional to the SNR and depend on the size of the observations window. In particular, the $\mathrm{CRVB}(\tau)$ is inversely proportional to W and depends on the number and the position of virtual subcarriers while, from (33), we can note that the $\mathrm{CRVB}(\Delta f)$ is inversely proportional to W^3.

Into the case of OFDM/OQAM systems substituting the transmitted signal model (1) in (31) and following the same reasoning reported in Appendix B, we obtain that the $\mathrm{CRVB}(\tau)$, $\mathrm{CRVB}(\Delta f)$ and $\mathrm{CRVB}(\phi)$ coincide with (32), (33) and (34), respectively.

V. Numerical Results

In this section the performance of the proposed joint LS and MLS symbol timing and CFO estimators is compared with that of the data-aided synchronization algorithms TR1 and TR2 proposed by Tonello and Rossi in [11]. As stated in section III all the considered symbol timing estimators require a maximization procedure with respect to the continuous parameter τ. In our simulations this maximization is performed

$$\boldsymbol{F} = \frac{2T_s}{\sigma_n^2}\begin{bmatrix} \dfrac{\partial \boldsymbol{s}(\tau)}{\partial \tau}\dfrac{\partial \boldsymbol{s}(\tau)^H}{\partial \tau} & \Re\left\{\dfrac{\partial \boldsymbol{s}(\tau)}{\partial \tau}\boldsymbol{D}_{\Delta f}\boldsymbol{s}(\tau)^H\right\} & \Re\left\{\dfrac{\partial \boldsymbol{s}(\tau)}{\partial \tau}\boldsymbol{D}_{\phi}\boldsymbol{s}(\tau)^H\right\} \\ \Re\left\{\dfrac{\partial \boldsymbol{s}(\tau)}{\partial \tau}\boldsymbol{D}_{\Delta f}\boldsymbol{s}(\tau)^H\right\} & -\boldsymbol{s}(\tau)\boldsymbol{D}_{\Delta f}^2\boldsymbol{s}(\tau)^H & -\boldsymbol{s}(\tau)\boldsymbol{D}_{\Delta f}\boldsymbol{D}_{\phi}\boldsymbol{s}(\tau)^H \\ \Re\left\{\dfrac{\partial \boldsymbol{s}(\tau)}{\partial \tau}\boldsymbol{D}_{\phi}\boldsymbol{s}(\tau)^H\right\} & -\boldsymbol{s}(\tau)\boldsymbol{D}_{\Delta f}\boldsymbol{D}_{\phi}\boldsymbol{s}(\tau)^H & -\boldsymbol{s}(\tau)\boldsymbol{D}_{\phi}^2\boldsymbol{s}(\tau)^H \end{bmatrix} \tag{31}$$

in two steps: in the first it is performed a coarse search with a step-size T_s followed, in the second step, by a parabolic interpolation.

A number of 10^4 Monte Carlo trials has been performed under the following conditions

1) The prototype filter is obtained by truncating the sampled version of an SRRC Nyquist filter with a rolloff factor α. Specifically, it is a FIR filter of length $N_g = 8K$ for FMT systems and $N_g = 4N$ for OFDM/OQAM systems.
2) The values of the normalized CFO $\Delta\nu = \Delta f T_s N$, of the normalized timing offset τ/T_s and of the carrier phase ϕ are uniformly distributed in $[-N/(4P), ..., N/(4P))$, $\{-N/2, ..., N/2 - 1\}$ and $[-\pi, ..\pi)$, respectively.
3) The values of the number of subcarriers and of the roll-off parameter for the considered FMT system are $N = 64$ and $\alpha = 0.125$, respectively.
4) The values of the number of subcarriers and of the roll-off parameter for the considered OFDM/OQAM system are $N = 64$ and $\alpha = 0.6$, respectively.
5) The multipath channel has been modeled to consist of $N_m + 1 = 5$ independent Rayleigh-fading taps with an exponentially decaying power delay profile. Specifically, $\mathrm{E}[|h(l)|^2] = Ce^{-l/4}$, $l \in \{0, \ldots, N_m\}$, where C is a constant such that $\sum_{l=0}^{N_m} \mathrm{E}[|h(l)|^2] = 1$. Moreover, the channel is fixed in each run but independent from one run to another.
6) The complex data symbols $a_p(l)$, when the FMT system is considered, belong to a QPSK constellation.
7) The data symbols $a_p^R(l)$ and $a_p^I(l)$, when the OFDM/OQAM system is considered, belong to a BPSK constellation.

A. OFDM/OQAM System

In this first set of simulations we have tested the performance of the considered algorithms for an OFDM/OQAM system in AWGN (solid lines) and multipath channel (dashed lines). Precisely, Figs 3 and 4 show the root mean squared error (RMSE) of the considered joint timing and CFO estimators, respectively, as a function of the SNR, for a training sequence with $N_{rip}^{OFDM/OQAM} = 2$ identical blocks each of length N. In Fig. 4 we have also shown the theoretical normalized RMSE of the LS CFO estimator whose derivation details are reported in the Appendix C. Moreover, in Figs 3 and 4 we have included the previously obtained Cramér-Rao bounds. As shown in Fig. 3 the TR2 symbol timing estimator exhibits the best performance for all the considered

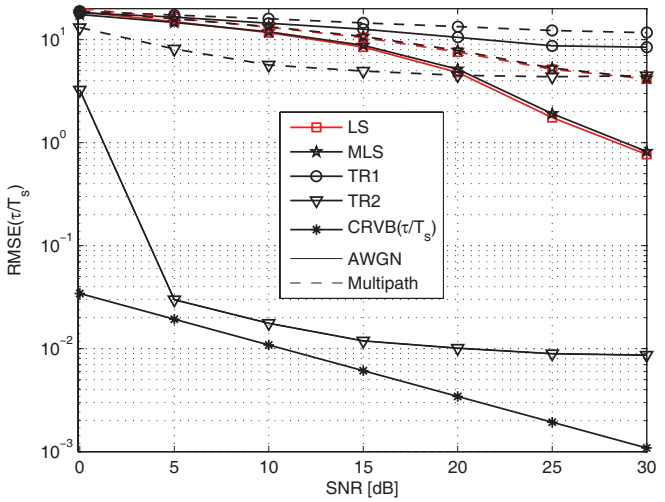

Fig. 3. Performance of the considered symbol timing estimators in AWGN (solid lines) and multipath channel (dashed lines) as a function of SNR and for an OFDM/OQAM system with $N = 64$ and $\alpha = 0.6$.

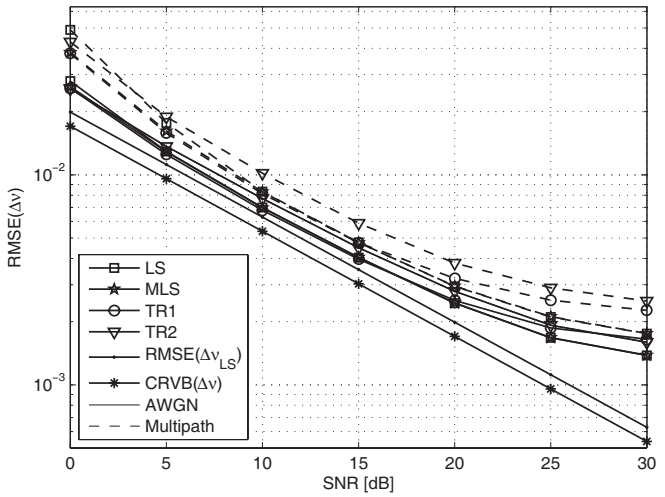

Fig. 4. Performance of the considered CFO estimators in AWGN (solid lines) and multipath channel (dashed lines) as a function of SNR and for an OFDM/OQAM system with $N = 64$ and $\alpha = 0.6$.

SNR values both in AWGN and multipath channel. However, in multipath channel and for sufficiently high SNR values, the proposed LS and MLS symbol timing estimators assure an RMSE nearly equal to that achieved by the TR2 estimator. On the other hand, as shown in Fig. 4, the TR2 CFO estimator provides the highest RMSE in multipath channel.

To gain some insight about the sensitivity of the OFDM/OQAM signal in terms of bit error rate (BER) on the

digital data to timing and carrier frequency offsets, in figures 5 and 6 is reported the BER of an OFDM/OQAM system with $N = 64$ subcarriers and SNR$=$ 10dB as a function of the timing offset (TO) normalized to the sampling interval (Fig.5) and as a function of the normalized CFO (Fig.6). Note that as observed in Section II, in the presence of frequency and timing synchronization errors at the output of each subchannel is observed an attenuation and a phase rotation of the useful data related to the subchannel index, the timing offset, the phase offset, the CFO and the index of the information symbol. The phase rotation incorporated in the channel gain should be compensated by the subcarrier equalizer. It is assumed that on each subchannel it is exploited a one-tap equalizer with perfect knowledge of the channel and, of the TO or of the CFO. The results reported in Fig.5 show that the sensitivity to a timing offset is lower in multipath channel and, moreover, in this case, an accuracy of ± 6 samples ($\simeq \pm 10\%$ of OFDM/OQAM symbol interval) is sufficient to assure a contained performance degradation with respect to the case of perfect synchronization. Moreover, as shown in Fig.6 in multipath channel the absolute value of the normalized CFO should be less than 5% to assure a reduced performance degradation. These results are in agreement with those in Fig.7 where it is reported the BER as a function of SNR both in AWGN and multipath channel. Specifically, in Fig.7 is reported the performance of the perfectly synchronized system and that obtained when the considered algorithms are exploited. The results show that in AWGN channel the adoption of the TR2 synchronization algorithm assures a performance quite similar to that obtained with perfect synchronization while, in multipath channel, and for sufficiently high values of SNR, the proposed LS and MLS algorithms can provide the best performance nearly coincident with that obtained in the absence of synchronization errors. Specifically, the performance cross-over is observed for SNR=20dB and is due to that fact that for SNR$\geq$ 20dB the performance of the timing estimators is quite similar while the LS and MLS CFO estimators outperform the TR2 estimator. It is worthwhile to emphasize that, the considered LS and MLS estimators exploit only the periodicity of the training burst while the TR2 estimator exploits also the knowledge of the periodic training burst.

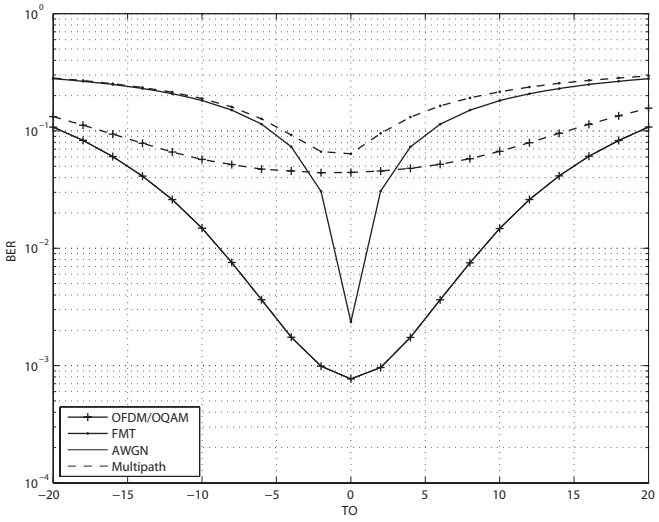

Fig. 5. BER of the considered FBMC systems as a function of the timing offset in AWGN (solid lines) and multipath channel (dashed lines) for SNR=10 dB.

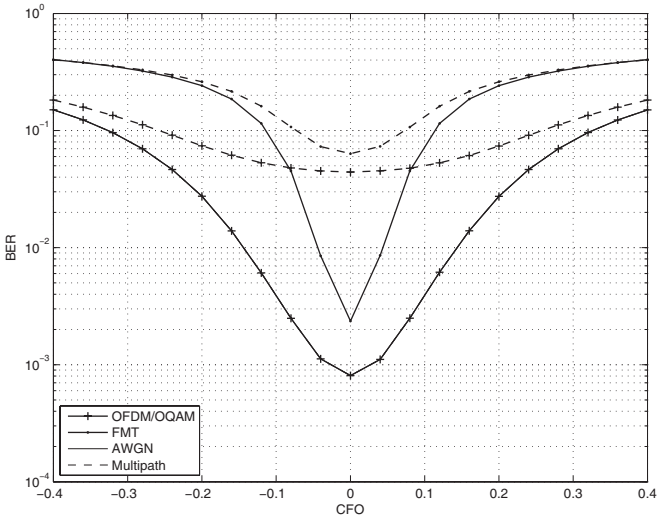

Fig. 6. BER of the considered FBMC systems as a function of the CFO in AWGN (solid lines) and multipath channel (dashed lines) for SNR=10 dB.

B. FMT System

In this subsection we present the performance of the considered algorithms for an FMT system in AWGN (solid lines) and multipath channel (dashed lines). Precisely, Figs 8 and 9 show the RMSE of the considered symbol timing and CFO estimators, respectively, as a function of the SNR for a training sequence containing two identical blocks of length $P - \gamma K$ where $P = lcm\{64, 72\} = 576$. We can note that both in AWGN and multipath channel the TR2 symbol timing estimator exhibits the best performance. In particular, in multipath channel the LS and MLS symbol timing estimators are expected to outperform the TR2 estimator only for very high values of SNR. In regard to the performance of the CFO estimators we can note that the LS and MLS estimators assure the lowest RMSE both in AWGN and multipath channel. Moreover, in multipath channel the TR2 CFO estimator provides the highest RMSE. However, for SNR$\geq$ 10dB the RMSE of the TR2 CFO estimator is lower than 0.1% and this accuracy is sufficient to assure a BER practically coincident with that of the perfectly synchronized system and lower than that obtained when the other considered synchronization algorithms are exploited (see Fig.10).

VI. Summary and Conclusions

In this paper the problem of data-aided symbol timing and CFO estimation in FBMC systems has been considered. In the first part of the paper we have investigated the sensitivity of FMT and OFDM/OQAM systems to synchronization errors. We have shown that the considered filter-bank based multicarrier systems are very sensitive to synchronization errors, in fact, as shown analytically, ISI and ICI can arise at the output of the subchanel matched filters at the receiver. Successively, a synchronization scheme based on a training sequence made up of identical parts has been considered. The proposed method

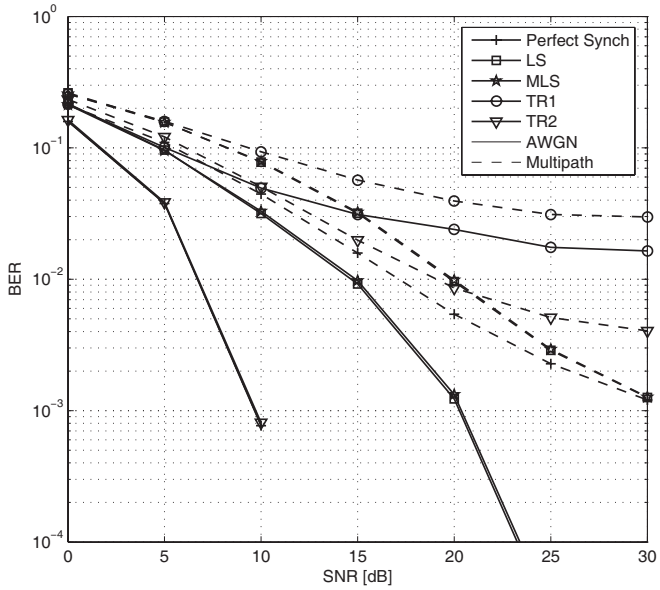

Fig. 7. BER of the considered joint CFO and symbol timing estimators in AWGN (solid lines) and multipath channel (dashed lines) as a function of SNR and for an OFDM/OQAM system with $N = 64$ and $\alpha = 0.6$.

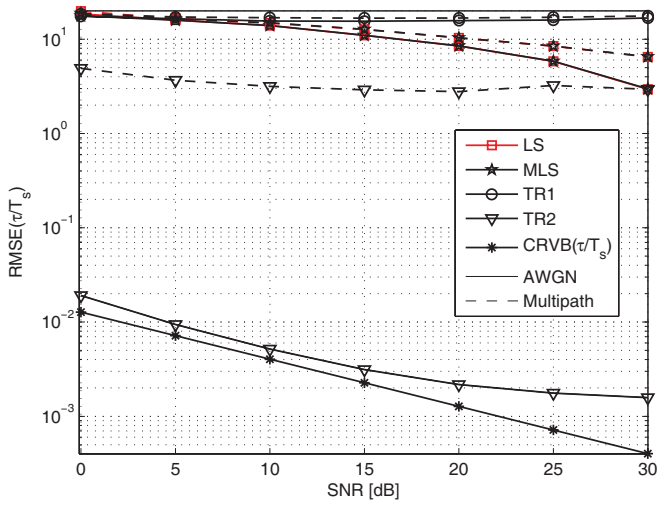

Fig. 8. Performance of the considered symbol timing estimators in AWGN (solid lines) and multipath channel (dashed lines) as a function of SNR and for an FMT system with $N = 64$ and $K = 72$.

is based on the LS approach, it operates in the time domain before running the receiver filter bank, and, moreover, it does not require the knowledge of the channel impulse response and of the SNR. The performance of the derived estimator has been assessed via computer simulation and compared with that of two joint symbol timing and CFO estimators previously proposed by Tonello and Rossi in [11] and referred to as TR1 and TR2. Specifically, the proposed estimators and the TR1 estimator exploit only the periodicity of the training burst while the TR2 joint estimator exploits also the knowledge of the periodic training burst. The numerical results have shown that the LS CFO estimator can outperform the TR2 estimator while the knowledge of the shape of the periodic training burst can be exploited by the TR2 to provide more accurate symbol timing estimates.

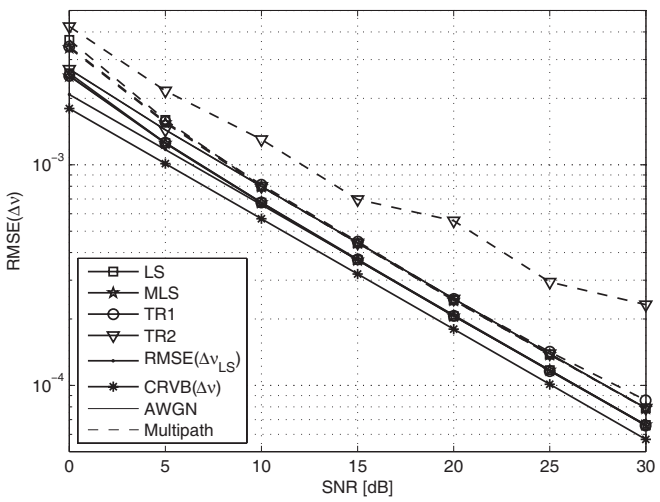

Fig. 9. Performance of the considered CFO estimators in AWGN (solid lines) and multipath channel (dashed lines) as a function of SNR and for an FMT system with $N = 64$ and $K = 72$.

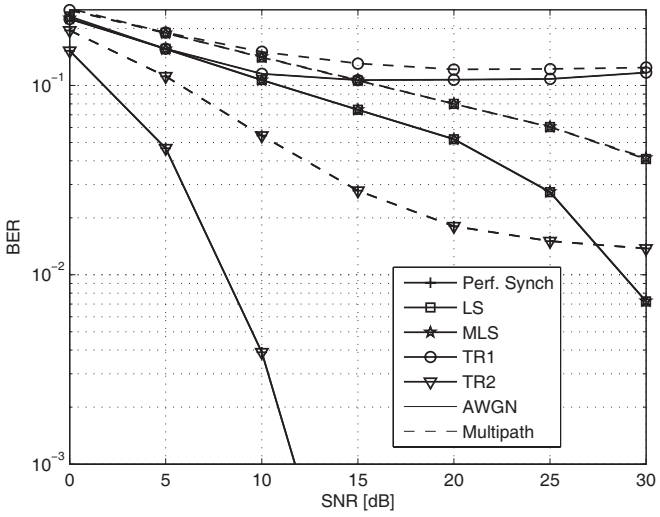

Fig. 10. BER of the considered joint CFO and symbol timing estimators in AWGN (solid lines) and multipath channel (dashed lines) as a function of SNR for an FMT system with $N = 64$ and $K = 72$.

APPENDIX A

In this Appendix, we illustrate how to derive the expression of the joint symbol timing and CFO LS estimator in (17) and (18). Let us consider the minimization problem in (16)

$$(\Delta\hat{f},\hat{\tau}) = \arg\min_{\Delta\tilde{f},\tilde{\tau}} \left\{ \sum_{k=N_g-1}^{N_{TR}N-P-1} |r(kT_s+\tilde{\tau}) - r(kT_s+PT_s+\tilde{\tau})e^{-j2\pi\Delta\tilde{f}T_sP}\Big|^2 \right\}$$

after simple algebraic manipulations we obtain

$$(\Delta\hat{f},\hat{\tau}) = \arg\min_{\Delta\tilde{f},\tilde{\tau}} \{Q_1(\tilde{\tau}) + Q_2(\tilde{\tau}) - 2|R(\tilde{\tau})|\cos(-2\pi\Delta\tilde{f}T_sP + \angle R(\tilde{\tau}))\} \quad (35)$$

with

$$Q_1(\tilde{\tau}) + Q_2(\tilde{\tau}) = \\ = \sum_{k=N_g-1}^{N_{TR}N-P-1} |r(kT_s+\tilde{\tau})|^2 + |r(kT_s+PT_s+\tilde{\tau})|^2$$

and

$$R(\tilde{\tau}) = \sum_{k=N_g-1}^{N_{TR}N-P-1} r^*(kT_s+\tilde{\tau}) r(kT_s+PT_s+\tilde{\tau}).$$

The maximum with respect to the CFO is obtained when the cosine term in (35) is equal to one. This yields the CFO estimator

$$\Delta\hat{f}(\tilde{\tau}) = \frac{1}{2\pi PT_s} \angle \{R(\tilde{\tau})\} \ .$$

In this case the cost function in (35) can be written as

$$\Gamma(\tilde{\tau}, \Delta\hat{f}(\tilde{\tau})) = \quad Q_1(\tilde{\tau}) + Q_2(\tilde{\tau}) - 2|R(\tilde{\tau})| \tag{36}$$

and the joint LS symbol timing and CFO estimator is given by

$$\hat{\tau}_{LS} = \arg\max_{\tilde{\tau}} \{2\,|R(\tilde{\tau})| - Q_1(\tilde{\tau}) - Q_2(\tilde{\tau})\}$$

and

$$\Delta\hat{f}_{LS}(\hat{\tau}_{LS}) = \frac{1}{2\pi PT_s} \angle \{R(\hat{\tau}_{LS})\} \ .$$

APPENDIX B

In this Appendix we present some algebraic details to derive the expression of the CRVB of joint symbol timing, CFO and phase offset estimation for FMT systems shown in (32), (33) and (34). Accounting for the expression of the transmitted FMT signal (10), the $(1,1)$ entry of FIM can be rewritten as

$$[\boldsymbol{F}]_{(1,1)} = \\ \frac{2T_sK}{\sigma_n^2} \sum_{k=N_g-1}^{N_{TR}N-1} \frac{1}{N_u} \Bigg[\sum_{l_1,l_2\in\mathcal{A}} a_{l_1} a_{l_2}^* e^{j\frac{2\pi(1+\alpha)}{T}[(kT_s-\tau)(l_1-l_2)]} \\ \times \sum_{p_1,p_2=-\infty}^{\infty} \frac{\partial g(kT_s-p_1KT_s-\tau)}{\partial\tau} \frac{\partial g(kT_s-p_2KT_s-\tau)}{\partial\tau} \\ + \frac{1}{N_u} \sum_{l_1,l_2\in\mathcal{A}} a_{l_1} a_{l_2}^* e^{j\frac{2\pi(1+\alpha)}{T}[(kT_s-\tau)(l_1-l_2)]} \frac{4\pi^2 l_1 l_2 (1+\alpha)^2}{T^2} \\ \times \sum_{p_1,p_2=-\infty}^{\infty} g(kT_s-p_1KT_s-\tau) g(kT_s-p_2KT_s-\tau) \Bigg] \ . \tag{37}$$

Under the assumption of a pulse shaping filter assumed to be an SRRC Nyquist filter with a signaling interval T we obtain

$$\sum_{p_1,p_2=-\infty}^{+\infty} g(kT_s-p_1T-\tau) g(kT_s-p_2T-\tau) \\ = \left(\sum_{p=-\infty}^{+\infty} g(kT_s-pT-\tau) \right)^2 \\ = \left(\int_{-\infty}^{+\infty} G(f) e^{j2\pi f(kT_s-\tau)} \sum_{p=-\infty}^{+\infty} e^{-j2\pi fpT} df \right)^2 \\ = \left(\frac{1}{T} \sum_{q=-\infty}^{+\infty} G\left(\frac{q}{T}\right) e^{j\frac{2\pi}{T}q(kT_s-\tau)} \right)^2 = \frac{1}{T} \tag{38}$$

and

$$\sum_{p_1,p_2=-\infty}^{\infty} \frac{\partial g(kT_s-p_1KT_s-\tau)}{\partial\tau} \frac{\partial g(kT_s-p_2KT_s-\tau)}{\partial\tau} = 0. \tag{39}$$

Therefore, we have

$$[\boldsymbol{F}]_{(1,1)} = \frac{2}{\sigma_n^2} \sum_{k=N_g-1}^{N_{TR}N-1} \\ \frac{1}{N_u} \sum_{l_1,l_2\in\mathcal{A}} a_{l_1} a_{l_2}^* e^{j\frac{2\pi(1+\alpha)}{T}[(kT_s-\tau)(l_1-l_2)]} \frac{4\pi^2 l_1 l_2 (1+\alpha)^2}{T^2} \ . \tag{40}$$

By exploiting the following result [15]

$$\frac{1}{W^q} \sum_{k=N_g-1}^{N_{TR}N-1} k^q \frac{1}{N_u} \sum_{l_1,l_2\in\mathcal{A}} a_{l_1} a_{l_2}^* e^{j\frac{2\pi(1+\alpha)}{T}[(kT_s-\tau)(l_1-l_2)]} l_1 l_2 \\ = \frac{1}{q+1} \frac{1}{N_u} \sum_{l\in\mathcal{A}} |a_l|^2 l^2 \\ + \mathcal{O}\left(\frac{1}{W^q}\right) \frac{1}{N_u} \sum_{\substack{l_1,\,l_2\,\in\,\mathcal{A} \\ l_1\,\neq\,l_2}} a_{l_1} a_{l_2}^* e^{j\frac{2\pi(1+\alpha)}{T}[(kT_s-\tau)(l_1-l_2)]} l_1 l_2 \\ \cong \frac{1}{q+1} \frac{1}{N_u} \sum_{l\in\mathcal{A}} |a_l|^2 l^2 \, . \tag{41}$$

and for a training sequence with $|a_l|^2 = 1 \ \forall l \in \mathcal{A}$, the expression (40) can be approximated by

$$[\boldsymbol{F}]_{(1,1)} = \frac{2W}{\sigma_n^2} \frac{1}{N_u} \sum_{l\in\mathcal{A}} \left(\frac{2\pi l(1+\alpha)}{T} \right)^2 \ . \tag{42}$$

Analogously, we obtain

$$[\boldsymbol{F}]_{(1,2)} = [\boldsymbol{F}]_{(2,1)} \\ = -\frac{4\pi^2 \mathrm{SNR}}{N_u N} (N_{TR}N - N_g + 1)(N_{TR}N + N_g - 3) \sum_{l\in\mathcal{A}} l \tag{43}$$

$$[\boldsymbol{F}]_{(1,3)} = [\boldsymbol{F}]_{(3,1)} = -\frac{4\pi \mathrm{SNR}}{TN_u} (N_{TR}N - N_g + 1) \sum_{l\in\mathcal{A}} l \tag{44}$$

$$[\boldsymbol{F}]_{(2,3)} = [\boldsymbol{F}]_{(3,2)} = \frac{2\pi}{\sigma_n^2} T_s (N_{TR}N - N_g)(N_{TR}N + N_g - 1) \tag{45}$$

$$[\boldsymbol{F}]_{(2,2)} = \frac{(2\pi T_s)^2}{\sigma_n^2} \frac{(N_{TR}N - N_g)}{3} \\ \times (2N_{TR}^2 N^2 + 2N_g^2 - 3N_{TR}N - 3N_g + 1 + 2N_g N_{TR} N) \tag{46}$$

$$[\boldsymbol{F}]_{(3,3)} = \frac{2}{\sigma_n^2} (N_{TR}N - N_g) \, . \tag{47}$$

The CRB for symbol timing and CFO is given by the corresponding diagonal element of inverse of FIM, that is

$$\mathrm{CRVB}\,(\tau) = \left[\boldsymbol{F}^{-1}\right]_{(1,1)} \\ = \frac{(NT_s)^2}{8\pi^2 W \mathrm{SNR} \left[\frac{1}{N_u} \sum_{l\in\mathcal{A}} \left(l - \frac{1}{N_u} \sum_{l\in\mathcal{A}} l \right)^2 \right]} \tag{48}$$

$$\mathrm{CRVB}(\Delta f) = \left[\boldsymbol{F}^{-1}\right]_{(2,2)} = \frac{3}{2(\pi T_s)^2 \mathrm{SNR}\, W^3} \tag{49}$$

$$\begin{aligned}\mathrm{CRVB}(\phi) &= \left[\boldsymbol{F}^{-1}\right]_{(3,3)} \\ &= \frac{3\left[4\beta\frac{1}{N_u}\sum_{l\in\mathcal{A}} l^2 - W^2\left(\frac{1}{N_u}\sum_{l\in\mathcal{A}} l\right)^2\right]}{2W^3\mathrm{SNR}\left[\frac{1}{N_u}\sum_{l\in\mathcal{A}}\left(l-\frac{1}{N_u}\sum_{l\in\mathcal{A}} l\right)^2\right]}\end{aligned} \tag{50}$$

APPENDIX C

In this Appendix we derive the theoretical variance of the LS, MLS, TR1 and TR2 CFO estimators reported in (18), (22), (24) and (26), respectively, in the case of perfect symbol timing synchronization. Let us observe that in the case of perfect symbol timing synchronization the LS and the TR1 CFO estimators are coincident and, moreover, for $|\hat{\Delta}f_{LS} - \Delta f| \ll 1/(2\pi P T_s)$ we can approximate their estimation error as (see [16])

$$\begin{aligned}\hat{\Delta}f_{LS} - \Delta f &\simeq \frac{1}{2\pi P T_s} \\ &\times \left\{ \frac{\sum_{k=N_g-1}^{N_{TR}N-P-1} \Im\left[e^{-j2\pi\Delta f P T_s} r^*(kT_s) r(kT_s + PT_s)\right]}{\sum_{k=N_g-1}^{N_{TR}N-P-1} \Re\left[e^{-j2\pi\Delta f P T_s} r^*(kT_s) r(kT_s + PT_s)\right]} \right\}.\end{aligned} \tag{51}$$

Substituting the signal model (2) in (51), under the assumption of high SNR conditions, we obtain

$$\begin{aligned}\hat{\Delta}f_{LS} - \Delta f &\simeq \frac{1}{2\pi P T_s \sum_{k=N_g-1}^{N_{TR}N-P-1} |s(kT_s)|^2} \\ &\times \sum_{k=N_g-1}^{N_{TR}N-P-1} \Im\left[w^*(kT_s)s(kT_s) + w(kT_s + PT_s)s^*(kT_s)\right]\end{aligned} \tag{52}$$

where, under the hypothesis of a zero-mean circular noise, the random variable

$$w(kT_s) \triangleq n(kT_s) e^{-j[2\pi\Delta f T_s k + \phi]}$$

is statistically coincident with $n(kT_s)$ and has a variance $\mathrm{E}[|w(kT_s)|^2] = \sigma_n^2/T_s$.

From (51) we obtain $E[(\hat{\Delta}f_{LS} - \Delta f)] = 0$, that is, for high SNR values the CFO LS estimate is unbiased. Moreover, the mean squared error is given by

$$E[(\hat{\Delta}f_{LS} - \Delta f)^2] = \frac{\sigma_n^2}{4\pi^2 P^2 T_s^3 \sum_{k=N_g-1}^{N_{TR}N-P-1} |s(kT_s)|^2}. \tag{53}$$

Note that, using the result (38) and the approximation (41), we have

$$\sum_{k=N_g-1}^{N_{TR}N-P-1} |s(kT_s)|^2 \simeq \frac{N_{TR}N - P - N_g + 1}{T_s}$$

therefore, the MSE in (53) can be approximated by

$$E[(\hat{\Delta}f_{LS} - \Delta f)^2] = \frac{1}{4\pi^2 P^2 T_s^2 \mathrm{SNR}(N_{TR}N - P - N_g + 1)}. \tag{54}$$

From (54) we can observe that, into the case of AWGN channel and perfect symbol timing synchronization the TR1 and LS CFO estimators have the same theoretical variance, whose expression depends on the length $N_{TR}N$ of the training sequence and it is inversely proportional to the SNR.

REFERENCES

[1] G. Cherubini, E. Eleftheriou, S. Ölçer, and J. M. Cioffi, "Filter bank modulation techniques for very high-speed digital subscriber lines," *IEEE Commun. Mag.*, vol. 38, pp. 98-104, May 2000.

[2] N. Benvenuto, S. Tomasin, and L. Tomba, "Equalisation methods in OFDM and FMT systems for broadband wireless communications," *IEEE Trans. Commun.*, vol. 50, no. 5, pp. 1016-1028, June 2002.

[3] T. Ihalainen, T. Hidalgo Stitz, M. Rinne, and M. Renfors, "Channel equalization in filter bank based multicarrier modulation for wireless communications," *EURASIP J. Applied Signal Processing*, vol. 2007.

[4] D. Lacroix, N. Goudard, and M. Alard, "OFDM with guard interval versus OFDM/offsetQAM for high data rate UMTS downlink transmission," in *Proc. VTC'01* Fall, Atlantic City, NJ, USA, Oct. 2001.

[5] P. K. Remvik and N. Holte, "Carrier frequency offset robustness for OFDM systems with different pulse shaping filters," in *Proc. GLOBECOM 1997*, vol. 1, pp. 11-15, Nov. 1997.

[6] T. Fusco, A. Petrella, and M. Tanda, "Sensitivity of multi-user filter-bank multicarrier systems to synchronization errors," in *Proc. ISCCSP 2008*, Malta, Mar. 2008.

[7] H. Bölcskei, "Blind estimation of symbol timing and carrier frequency offset in wireless OFDM systems," *IEEE Trans. Commun.*, vol. 49, pp. 988-999, June 2001.

[8] T. Fusco and M. Tanda, "Blind frequency-offset estimation for OFDM/OQAM systems," *IEEE Trans. Signal Processing*, vol. 55, pp. 1828-1838, May 2007.

[9] T. Fusco, A. Petrella and M. Tanda, "Non-data-aided carrier-frequency offset estimation for pulse shaping OFDM/OQAM systems," *Signal Processing*, vol. 88, pp. 1958-1970, Aug. 2008.

[10] T. Fusco, A. Petrella, and M. Tanda, "Blind CFO estimation for non-critically sampled FMT systems," *IEEE Trans. Signal Processing*, vol. 56, pp. 2603-2608, June 2008.

[11] A. Tonello and F. Rossi, "Synchronization and channel estimation for filtered multitone modulation," in *Proc. WPMC 2004*, Abano Terme, pp. 590-594, Sept. 2004.

[12] T. H. Stitz, T. Ihalainen, and M. Renfors, "Practical issues in frequency domain synchronization for filter bank based multicarrier transmission," in *Proc. ISCCSP 2008*, Malta, Mar. 2008.

[13] H. Minn, V. K. Bhargava, and K. B. Letaief, "A robust timing and frequency synchronization for OFDM systems," *IEEE Trans. Wireless Commun.*, vol. 2, pp. 822-839, July 2003.

[14] COST 207, "Digital land mobile radio communications," Office for Official Publications of the European Communities, Final Report, Luxemburg, 1989.

[15] P. Stoica, T. Söderström, and F. N. Ti, "Asymptotic properties of the high-order Yule-Walker estimates of sinusoidal frequencies," *IEEE Trans. Acoustics Speech Signal Processing*, vol. 37, pp. 1721-1734, Nov. 1989.

[16] P. H. Moose, "A techique for orthogonal frequency division multiplexing frequency offset correction," *IEEE Trans. Commun.*, vol. 42, pp. 2908-2914, Oct. 1994.

Tilde Fusco was born in Napoli, Italy, on March 22, 1977. She received the Dr. Eng. degree (summa cum laude) in electronic engineering from the Second University of Napoli in 2002 and the Ph.D. degree in electronic and telecommunication engineering from the University of Napoli Federico II in 2006. From November 2005 to June 2006, she was with the CNIT national laboratory of multimedia communication of Napoli, and from July 2006 to March 2007, she was awarded a scholarship by the CRdC-ICT of Benevento. Since April 2007, she has been a Research Assistant with the Department of Electronics and Telecommunications Engineering, University of Napoli Federico II. Her current research and study interests lie in the area of statistical signal processing, with emphasis on parameter estimation problems in the context of multicarrier systems.

Angelo Petrella was born in Formia, Italy on February 24, 1983. He received the Dr. Eng. Degree (summa cum laude) in Telecommunications Engeneering from the University of Naples Federico II in 2006. Currently he is a PhD student at the Department of Biomedical, Electronics and Telecommunications Engeneering of the University of Naples Federico II. His area of interest concerns statistical signal processing, with emphasis on parameter estimation problems in the context of filterbank multicarrier transmissions.

Mario Tanda was born in Aversa, Italy, on July 15, 1963. He received the Dr. Eng. degree (summa cum laude) in electronic engineering in 1987 and the Ph.D. degree in electronic and computer engineering in 1992, both from the University of Napoli Federico II. Since 1995, he has been an Appointed Professor of Signal Theory at the University of Napoli Federico II. Moreover, he has been an Appointed Professor of Electrical Communications (from 1996 until 1997) and Telecommunication Systems (from 1997 until 2008) at the Second University of Napoli. He is currently a Full Professor of Telecommunications at the University of Napoli Federico II. His research activity is in the area of signal detection and estimation, multicarrier, and multiple access communication systems.